A wavelength-selective add-drop switch using silicon microring resonator with a submicron-comb electrostatic actuator

Kazunori Takahashi,[1] Yoshiaki Kanamori,[1] Yasuo Kokubun,[2] and Kazuhiro Hane[1,*]

[1]*Department of Nanomechanics, Tohoku University, Sendai 980-8579, Japan*
[2]*Graduate School of Engineering, Yokohama National University, Yokohama 240-8501, Japan*
[*]*Corresponding author: hane2@hane .mech.tohoku.ac.jp*

Abstract: Electrostatic comb-drive micro actuator with submicron comb fingers was connected to silicon microring resonator to consist a wavelength-selective add-drop switch at 1.5μm wavelength with variable coupling mechanism. A 500nm wide 260nm thick 63.4μm long silicon microring waveguide was suspended in air with low-loss suspension arms. The air gap between the microring and the input/output waveguides was adjusted by the voltage applied to the comb actuator to vary the coupling efficiency. Transmittance from the input port to a drop port was varied 32.9dB by applying the voltages from 0V to 28.2V. At 28.2V, transmittance from the input port to a through port decreased by 7.83dB from that at 0V, and 55% of the intensity was transmitted to the drop port. The full-width-half-maximum bandwidth of the dropped light was 0.5nm, corresponding to a Q-value of 3150.

OCIS codes: (230.4685) Optical microelectromechanical devices, (130.7408) Wavelength filtering devices, (250.5300) Photonic integrated circuits.

References and links

1. B. Jalali and S. Fathpour, "Silicon photonics," J. Lightwave Technol. **24,** 4600-4615 (2006).
2. H. Yamada, T. Chu, S. Ishida, Y. Arakawa, "Si photonic wire waveguide devices," IEEE J. Sel. Topics Quantum Electron. **12,** 1371-1379 (2006).
3. A. Sasaki, G. Hara, T. Baba, "Propagation characteristics of ultrahigh-Δ optical waveguide on silicon-on-insulator substrate," Jpn. J. Appl. Phys. **40,** L383-L385 (2001).
4. W. Bogaerts, P. Dumon, D.V. Thourhout, D. Taillaert, P. Jaenen, J. Wouters, S. Beckx, V. Wiaux, R. G. Baets, "Compact wavelength-selective functions in silicon-on-insulator photonics wires," IEEE J. Sel.Topics Quantum Electron. **12,** 1394-1401 (2006).
5. K. Sasaki, F. Ohno, A. Motegi, T. Baba, "Arrayed waveguide grating of 70x60μm^2 size based on Si photonic wire waveguides," Electron. Lett. **41,** 801-802 (2005).
6. A. Vorckel, M. Monster, W. Henschel, P. H. Bolivar, H. Kurz, "Asymmetrically coupled silicon-on-insulator microring resonators for compact add-drop multiplexers," IEEE Photon. Technol. Lett. **15,** 921-923 (2003).
7. E. Bulgan, Y. Kanamori, K. Hane, "Submicron silicon waveguide optical switch driven by microelectromechanical actuator," Appl. Phys. Lett. **92,** 101110 (2008).
8. A. Liu, R. Jones, L. Liao, D. Samara-Bublo, D. Rubin, O. Cohen, R. Nicolaescu, M. Paniccia, "A high-speed silicon optical modulator based on a metal-oxide-semiconductor capacitor," Nature, **427,** 615-618 (2004).
9. C. Gunn, "CMOS photonics for high-speed interconnects," IEEE Micro, **26,** 58-66 (2006).
10. T. Kato, S. Suzuki, Y. Kokubun, S. T. Chu, "Coupling-loss reduction of a vertically coupled microring resonator filter by spot-size matched busline waveguide," Appl. Opt. **41,** 4394-4399 (2002).
11. T. Ito, Y. Kokubun, "Nondestructive measurement of propagation loss and coupling efficiency in microring resonator filters using filter responses," Jpn. J. Appl. Phys. **43,** 1002-1005 (2004).
12. Y. Goebuchi, T. Kato, Y. Kokubun, "Fast and stable wavelength-selective switch using double-series coupled dielectric microring resonator," IEEE Photon. Technol. Lett. **18,** 538-540 (2006).
13. W. M. J. Green, R. L. Lee, G. A. DeRose, A. Scherer, A. Yariv, "Hybrid InGaAsP-InP Mach-Zehnder racetrack resonator for thermooptic switching and coupling control," Opt. Express **13,** 1651-1659 (2005).
14. U. Levy, K. Campbell, A. Groisman, S. Mookherjea, Y. Fainman, "On-chip microfluidic tuning of an optical microring resonator," Appl. Phys. Lett. **88,** 11107 (2006).

#99264 - $15.00 USD Received 23 Jul 2008; revised 25 Aug 2008; accepted 26 Aug 2008; published 29 Aug 2008

15. T. J. Wang, C. H. Chu, C. Y. Lin, "Electro-optically tunable microring resonators on lithium niobate," Opt. Lett. **32,** 2777-2779 (2007).
16. K. E. Moselund, P. Dainesi, M. Declercq, M. Bopp, P. Coronel, T. Skotnicki, A. M. Ionescu, "Compact gate-all-around silicon light modulator for ultra high speed operation," Sensors Actuators A, **130-131,** 220-227 (2006).
17. G. Sekiguchi, N. Kobayashi, Y. Kokubun, "Coupling efficiency control of vertically coupled microring resonator filter by microactuator," IEEE Photon. Technol. Lett. **18,** 2141-2143 (2006).
18. J. Yao, D. Leuenberger, M. M. Lee, M. C. Wu, "Silicon microtoroidal resonators with integrated MEMS tunable coupler," IEEE Sel. Topics Quantum Electron. **13,** 202-208 (2007).
19. T. Fukazawa, T. Hirano, F. Ohno, T. Baba, "Low loss intersection of Si photonic wire waveguides," Jpn. J. Appl. Phys. **43,** 646-647 (2004).
20. L. Martines and M. Lipson, "High confinement suspended micro-ring resonators in silicon-on-insulator," Opt. Express **14,** 6259-6263 (2006).
21. Y. Fukuta, H. Fujita, H. Toshiyoshi, "Vapor hydrofluoric acid sacrificial release technique for micro electro mechanical systems using labware," Jpn. J. Appl. Phys. **42,** 3690-3694 (2003).
22. K.Okamoto, *Fundamentals of optical waveguides*. Tokyo, Corona Press, pp.158-165 (1996).

1. Introduction

Submicron silicon waveguides are promising for dense integration of optical circuits with silicon electronics in the fields of optical telecommunications and interconnects [1]. Several devices using submicron silicon waveguides were proposed [2-7]. In addition to a simple bent waveguide [3], functional devices such as waveguide couplers [2], filters [4-6] and optical switches [2,7], etc. were studied. The recent reports on silicon optical modulator and receiver have also attracted increasing attention to silicon photonic-electronic integration [8,9].

As an efficient narrow band filter, microring resonators have been studied intensively [4, 6, 10, 11]. Wavelength-selective add-drop switch is a promising application of the microring resonator filter. A wavelength-channel-selective switch has been demonstrated using thermooptic effect of double series-coupled microring resonators [12]. Due to use of double microrings, each channel can be switched without disturbing other ones while maintaining the microring coupling gap with busline. In order to construct a wavelength-selective switch using microring resonators, a mechanism for controlling the coupling between the microring and busline is needed in addition to the wavelength tuning. Although several techniques for tuning the resonant wavelength of microring such as thermooptic effect [13], fluid insertion [14], electrooptical effects [15,16] have been proposed, there are only few reports on the control of the coupling between the microring and busline.

Micro-electro-mechanical systems (MEMS) technology is also attractive for controlling the coupling efficiency [17,18]. A silicon microtoroidal resonator with integrated MEMS tunable coupler was reported [18]. A high Q-value (5400-110000) and a wide tuning range (22.4dB extinction ratio) of waveguide coupling were obtained. One complication came from making the microdisk in toroidal shape to improve Q-value and the wafer bonding process was used to integrate vertical actuators.

In this paper, a wavelength-selective add-drop switch using a silicon microring resonator is reported, in which the coupling between busline and microring is variable by an electrostatic micro comb actuator. A microring resonator is suspended in air by connecting to an actuator with low-loss suspension arms. All parts of the device are fabricated on top layer of silicon on insulator (SOI) wafer using a single electron beam mask process. The optical properties of the proposed device have been experimentally measured.

2. Device design, fabrication and experiments

Figures 1(a) and 1(b) show the schematic diagrams of the proposed wavelength-selective add-drop switch using a microring resonator combined with a microactuator. The coupling between the microring and buslines can be changed by the microring movement. The input light is selectively transmitted to the drop port when the microactuator makes the microring approach to the buslines under the condition that the input wavelength is equal to one of the resonant wavelengths of the microring. On the other hand, when the actuator is not operated, the microring is apart from the buslines so as to decrease the coupling efficiency. The input

#99264 - $15.00 USD Received 23 Jul 2008; revised 25 Aug 2008; accepted 26 Aug 2008; published 29 Aug 2008

light passes to the through port without interacting with the microring resonator. Therefore, the proposed device works as a wavelength-selective add-drop switch.

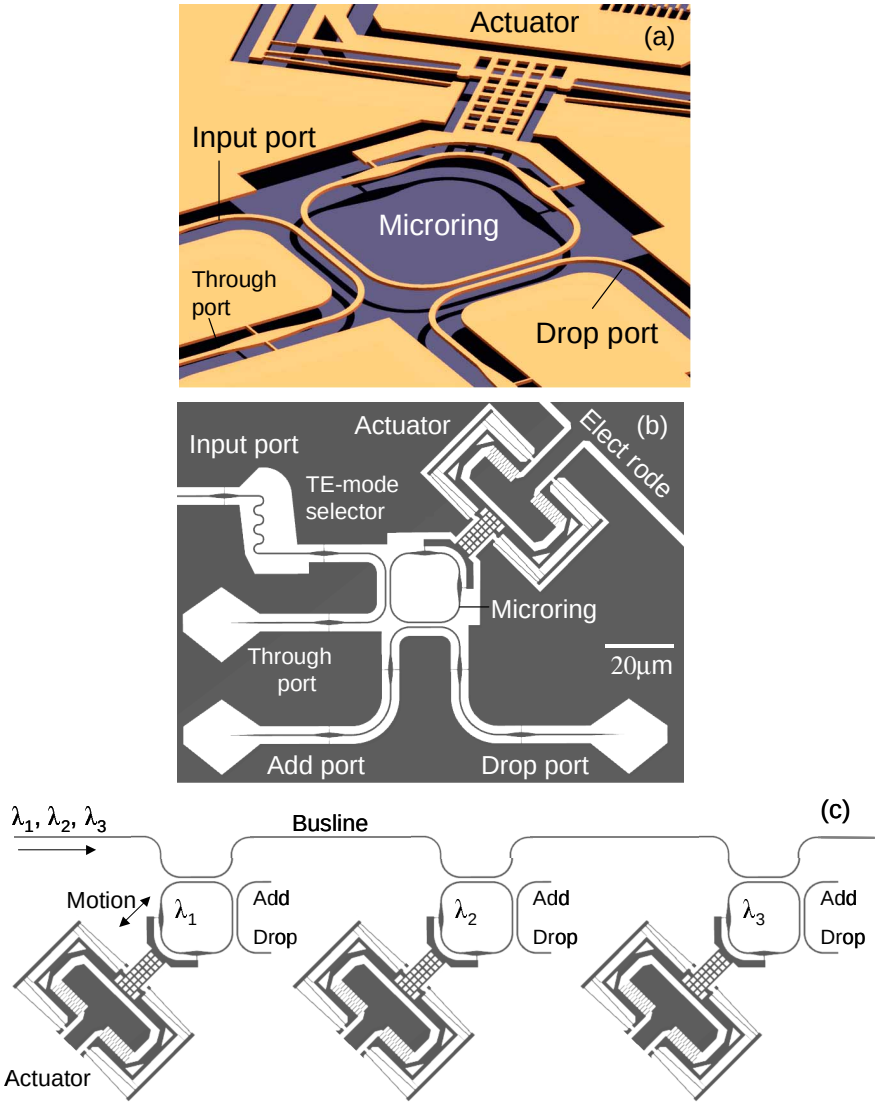

Fig. 1. (a). Schematic diagram of microring resonator wavelength-selective add-drop switch with a microactuator, (b) Actual arrangement of the device components, (c) An application of the proposed device for the wavelength division multiplex system.

As shown in Fig. 1(a), the proposed device consists of three submicron silicon waveguides i.e. two buslines and a microring resonator. One busline waveguide is used as an input port and a through port. The other busline waveguide is for a drop port and an add port. The two busline waveguides are bent to an angle of 90 degrees with a bent waveguide having the radius of 5μm to be located closely to the microring waveguide as shown in Fig. 1(a). The microring resonator is a closed loop rounded square waveguide with four 5μm radius corners. Those waveguides are 500nm wide and 260nm thick, which is designed as a single-mode waveguide based on waveguide mode equation analysis. The lowest TM mode wave is eliminated experimentally by a TE-mode selector. The round trip length of the microring resonator is 63.4μm. The region of the microring waveguide parallel to the buslines is 8μm

#99264 - $15.00 USD Received 23 Jul 2008; revised 25 Aug 2008; accepted 26 Aug 2008; published 29 Aug 2008

long, and the initial gap between the ring and the buslines is 775nm. All the waveguides are supported in air by the suspension bridges. In order to minimize the optical loss generated by the suspension bridge, a tapered profile for the increase in the waveguide geometry is used in the elliptical bridge [19,20] as shown in Fig. 1(a). It was recently reported that a silicon microring resonator supported in air by two suspension bridges was fabricated from SOI wafer by silicon micromaching, and the Q-value as high as 15000 was obtained [20]. The elliptical bridge is 8μm long and 1.5μm wide, and the suspension arm is 200nm wide and 1μm long in the designed patterns.

The electrostatic comb-drive actuator is used to translate the suspended microring. The area of the actuator is 25μm wide and 50μm long. The comb finger is 250nm wide, 260nm thick, and 2μm long, and the gap between each finger pair is 350nm. The comb area is 2.5μm wide and 8μm long. Doubly folded springs are utilized in the microactuator. Each of the spring elements is a straight silicon bar with the width of 250nm, the thickness of 260nm and the length of 17.5μm, which corresponds to an equivalent spring constant of 0.23N/m.

Figure 1(b) illustrates the actual arrangement of the components of the proposed device. The fixed comb of the actuator is connected to an electrode for the application of voltage. In addition to the microring and the busline waveguides, the input and output waveguides are connected for measurement. The input light is introduced into the input port through a bent waveguide to eliminate TM-mode. The through and drop waveguides are narrowed at their ends for suppressing the reflection. The output light intensities at the through and drop ports are measured from the spot image intensity of the scattered light at the ends of the narrowed waveguides using an infrared (IR) camera (Goodrich SU320KTS-1.7RT). The gamma value of the IR camera was calibrated to be 1.0. The uniformity of the camera image was better than 1% in the intensity evaluation. Although the emissions from the narrowed ends of the waveguides were directional, the detection efficiencies normal to the substrate were equal for the respective output ports because of the symmetry of the optical arrangement. A tunable laser (Agilent 81682A) was used as a light source in the experiment. For coupling the tunable laser light to the fabricated device, a lensed single-mode fiber was used to focus the laser light on the end surface of the waveguide. The facet of the input waveguide was obtained by cleaving the silicon wafer from the backside on which a shallow groove was diced.

Figure 1(c) depicts a possible application of the proposed devices in the wavelength division multiplex system. As an example, the input light at the wavelengths of λ_1, λ_2 and λ_3 are selectively dropped by the respective switches using microrings having the resonant wavelengths of λ_1, λ_2 and λ_3.

In the fabrication of the designed device, electron beam lithography was utilized. A SOI wafer with a 260nm thick top silicon layer and a 2.0μm SiO_2 layer was used. The top silicon layer was used for the waveguide and the actuators. The SiO_2 layer was etched sacrificially to make the actuator movable. After cleaning the wafer, a 350nm thick positive resist (ZEON Co.Ltd. ZEP-520A) was coated. The coated resist was exposed by electron beam at the dose around 77.6μC/cm^2. After the development of the resist, the top silicon layer was etched by a fast atom beam from a DC SF_6 gas plasma (Ebara FAB-60ML). The etching ratio between the polymer resist and silicon layer was 0.73 at the etching rate of 16nm/min. Finally, the hydrofluoric acid vapor generated by heating the solution was used to etch the SiO_2 layer underneath the etched top silicon layer [21].

In the calculation, finite difference time domain (FDTD) method (Crystalwave Co. Ltd.) was used for simulating the fundamental functions of the proposed device. Due to the limitations imposed by calculation time and memory size, a continuous wave at a given wavelength was used for the calculations. For the simple 90-degree bend waveguide used in the microring, the calculated loss was negligible compared to the output light intensity as reported in Ref. 3. The transmission loss of the elliptical bridge was calculated to be about 0.11dB. Wavelength dependence of the microring filter was calculated using the mode coupling equations for microring resonator [22] due to the aforementioned limitation.

#99264 - $15.00 USD Received 23 Jul 2008; revised 25 Aug 2008; accepted 26 Aug 2008; published 29 Aug 2008

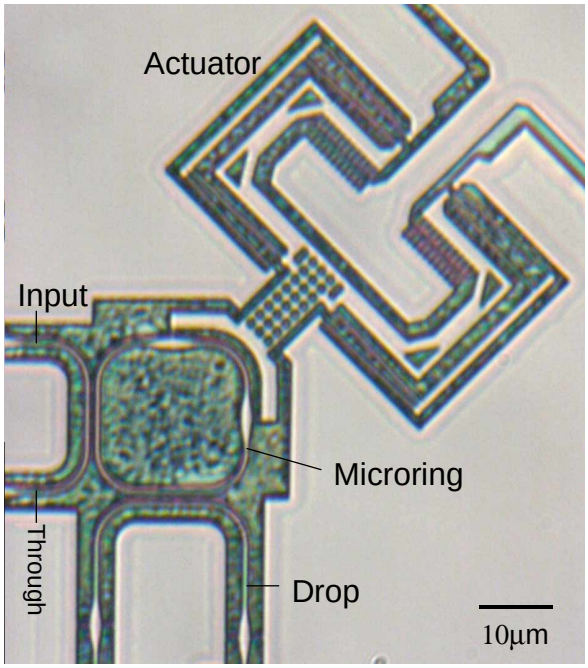

Fig. 2. Optical micrograph of the fabricated microring wavelength-selective add-drop switch.

3. Results and discussion

Figure 2 shows the optical micrograph of the whole view of the fabricated device. The submicron silicon waveguides and the electrostatic comb actuator are properly fabricated, and they are suspended in air although the springs and comb are too thin to be imaged by the optical microscope. Although the top Si layer of SOI wafer suffered residual stress from wafer bonding, the fabricated structures did not deflect very much since the structures were designed not to be affected by the residual stress. The actuator surface was scanned with a laser beam of an optical surface profiler to obtain the height distribution. The maximum height difference obtained in the actuator region was less than 50nm, which is smaller than the thickness of waveguide 260nm. Thus, the influence of the height difference on the optical performance was not considered significant. The levitation was generated if a simple structure like a cantilever was fabricated. The doubly folded spring decreased the levitation since the moving part is connected close to the fixed point of the spring. Moreover, the fixed end of the spring was connected to a square corner of the etched region, where the deflection of the top silicon layer was minimized. The force and displacement generated by the micro actuator were approximately 1.5×10^{-7} N and 0.63μm, respectively at the voltage of 28V.

The channel drop experiment was carried out using the fabricated device. Figures 3(a)-3(d) show the IR camera images obtained in the experiments. Figure 3(a) shows the device image before the incidence of the laser light. The microring, the actuator and the respective ports are imaged in the dark background. As shown in Fig. 3(b), a bright light spot is observed at the drop port under the condition that 50μW laser light is incident on the input port at the microring resonant wavelength of 1557.94nm, and the actuator is activated at the voltage of 28.2V (i.e. on-state of the switch). A small spot at the through port is also observed. Therefore, the drop efficiency is larger than the through efficiency at the ON state. In the observed image, slightly scattered light is seen at the suspension arms of the ring.

#99264 - $15.00 USD Received 23 Jul 2008; revised 25 Aug 2008; accepted 26 Aug 2008; published 29 Aug 2008

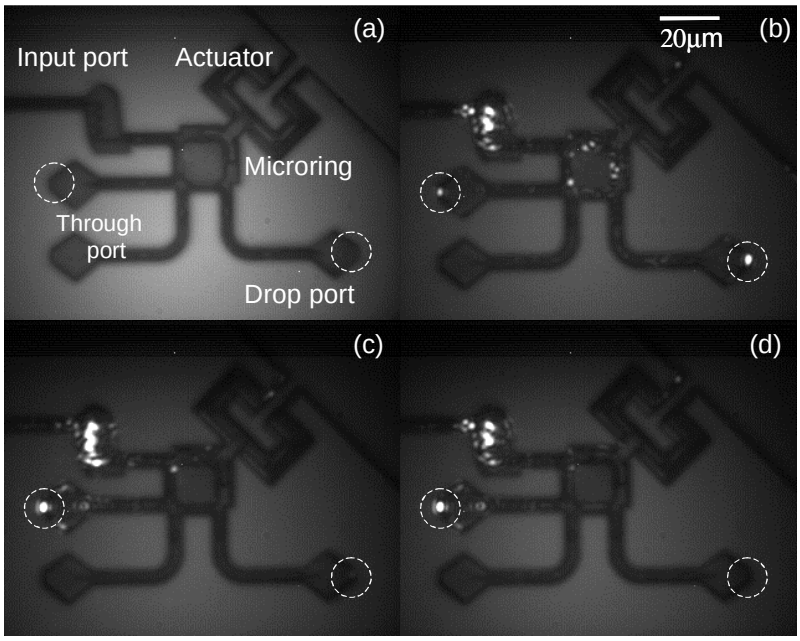

Fig. 3. Infrared camera images, (a) microring switch without input light, (b) with 1557.94nm resonant input light at the actuator voltage of 28.2V, (c) with 1556.94nm off-resonant input light at 28.2V, (d) with 1557.94nm resonant input light at 0V.

Figure 3(c) shows the IR image of the device under the conditions that 50μW laser light at the off-resonant wavelength of 1556.94nm is incident on the input port and the actuator is activated at the voltage of 28.2V. Although the actuator is at the ON state, the incident light is not transmitted to the drop port since the wavelength of the laser is not equal to the resonant wavelength of the microring. A bright spot of the laser light is observed at the through port without interacting with the microring.

Figure 3(d) shows the image obtained without applying the voltage (i.e. OFF state of the switch) under the condition that the same laser light used in the measurement of Fig. 3(b) at the resonant wavelength of 1557.94nm is incident on the input port. Since the distance between the microring and the busline is too large to interact with each other, the lightwave is not transmitted to the drop port even if the wavelength is equal to a resonant wavelength of the microring.

Quantitative optical properties of the fabricated device were also investigated for other devices with the same structure. Figure 4(a) shows the drop efficiency measured as a function of the input laser wavelength. The drop efficiency is obtained from the spot intensities of the IR images at the through port under the OFF state of the switch and at the drop port under the ON state assuming that the through intensity at OFF state is equal to the input intensity immediately anterior to the microring. The free spectral range (FSR) was 8.45nm, and the effective index was calculated to be 4.60, which was consistent with the formally reported value [3]. Since the peak width at the wavelength of 1576nm is approximately 0.5nm, the Q-value is about 3150. The maximum change in the drop intensity between the resonant and off-resonant conditions is approximately 21dB in Fig. 4(a).

In addition, we carried out theoretical calculation using the mode coupling equations for the microring resonator [22]. Using the effective index of 4.6 and the coupling coefficient of 0.103 obtained experimentally as described below, the dropping efficiency was obtained as a function of wavelength. The calculation result is shown by the solid curve in Fig. 4(a), which explains roughly the experimental results and shows that FSR is 8.2nm.

#99264 - $15.00 USD Received 23 Jul 2008; revised 25 Aug 2008; accepted 26 Aug 2008; published 29 Aug 2008

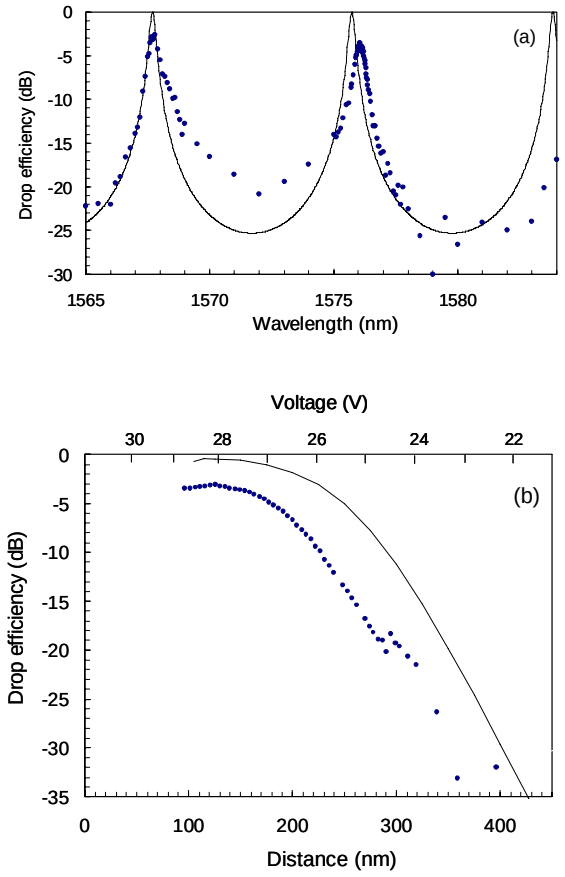

Fig. 4. (a). Drop efficiency measured as a function of the wavelength at the voltage of 28.2V, (b) drop efficiency measured as a function of the applied voltage at the resonant wavelength of 1576.04nm. The solid curves show the calculation results.

Figure 4(b) shows the drop efficiency at the resonant wavelength of 1576.04nm measured as a function of the distance between the microring and busline. The air gap was experimentally determined from the displacement of the actuator measured as a function of voltage in the scanning electron microscope chamber. The corresponding voltage is also plotted in Fig. 4(b). By decreasing the distance from the initial position (775nm), the dropped light started to increase around 300nm, and steeply increased between 300 to 120nm. By further approaching to the busline, the drop efficiency decreased slightly. The range of the actuator displacement is limited by the contact of the waveguides if the voltage is further increased. The critical coupling occurs at the gap of 120nm since the maximum intensity is obtained as a function of the gap.

In addition, we carried out theoretical calculation using FDTD method. The calculated drop efficiency is as shown in Fig. 4(b). The relative dependence of the experimental values can be explained by the calculation. The difference in the absolute values between the measurement and the calculation may be caused by the fabrication errors.

In the tested devices, the maximum drop efficiency was –2.59dB (55% transmission) under the resonant condition (1557.94nm), and the through efficiency was –7.83dB (16.5%

#99264 - $15.00 USD Received 23 Jul 2008; revised 25 Aug 2008; accepted 26 Aug 2008; published 29 Aug 2008

transmission). The rest power loss of 28.5% (–5.47dB) seems to be attributed to the losses by the suspension arms. Since the ON resonance transmission efficiency of through port was 7.83dB, and the full-width-half-maximum bandwidth was 0.5nm, the coupling efficiency at ON state and the round trip loss of resonator were evaluated to be 0.103 and 0.62 dB/round, respectively, using formulas given in Ref. 11. By comparing the drop intensities between the OFF and ON states, maximum change in the dropped light intensity was found to be 32.9dB. By improving the geometries of microring and suspension arms as well as fabrication precision, the total switch loss can be decreased. Modifying the design of coupling structure such as asymmetric coupling [6], the extinction ratio at the through port can be improved.

4. Conclusion

A 500nm wide, 260nm thick, and 63.4μm long silicon microring waveguide was suspended in air by connecting to an electrostatic microactuator. The coupling efficiency between the microring and the busline was adjusted by the actuator. The maximum drop efficiency was -2.59dB of the input intensity, which corresponded to the dropped light intensity change of 32.9dB by moving the actuator. Since the fabrication procedure is simple, the proposed switch can be easily combined with other novel silicon waveguide devices.

Acknowledgments

This work was supported by a Grant-in-Aid for Scientific research (17068002).

#99264 - $15.00 USD Received 23 Jul 2008; revised 25 Aug 2008; accepted 26 Aug 2008; published 29 Aug 2008